Ephrin-A5 restricts topographically specific arborization in the chick retinotectal projection *in vivo*

Takashi Sakurai*†, Eric Wong*‡, Uwe Drescher§¶, Hideaki Tanaka‖, and Daniel G. Jay*,

*Department of Physiology, Tufts University School of Medicine, Boston, MA 02111; §Department of Physical Biology, Max Planck Institute for Developmental Biology, Spemannstrasse 35, FRG-72076 Tübingen, Germany; and ‖Division of Developmental Neurobiology, Department of Neuroscience, Kumamoto University Graduate School of Medical Sciences, Kuhonji, Kumamoto 862, Japan

Edited by Charles F. Stevens, The Salk Institute for Biological Studies, La Jolla, CA, and approved June 18, 2002 (received for review March 19, 2002)

The retinotectal map is the best characterized model system to study how axons respond to guidance cues during the formation of the nervous system. Recent studies have shown that the critical event in forming this map is topographic-specific axon branching. To elucidate the *in vivo* role of the repulsive cue ephrin-A5 in this event, we used chromophore-assisted laser inactivation (CALI) to generate acute loss of ephrin-A5 function in localized areas of the posterior tectum of chick embryos *in ovo* and analyzed the resulting changes of retinal projections during initial outgrowth (E11) and when retinal axons arborize in the deep layers in the tectum (E12). We confirmed that ephrin-A5 functions to restrict initial axon outgrowth at E11. At E12, CALI of ephrin-A5 did not affect the extent of axon outgrowth on the tectal surface but instead caused ectopic arborization posterior to the topographically correct site in deeper layers of the tectum. This shows that ephrin-A5 restricts arborization during this critical process for developing the retinotopic map. CALI provides an approach to inactivate *in vivo* function in higher vertebrates with high temporal and spatial specificity that may have wide application.

The retinotectal projection is a well established model system to study mechanisms that form the topographic map of neural connections in the brain. It is thought that molecules expressed in gradients guide axons to their precise topographic targets. This chemoaffinity hypothesis proposed by Sperry (1) has been supported by the identification of molecular cues expressed in gradients in the retina and in the tectum (2). One important guidance cue is ephrin-A5 (3). The graded expression of ephrin-A ligands in the tectum coupled with expression of the Eph receptors that bind these ligands in retinal axons provides a potential molecular mechanism for defining the anterior–posterior (A–P) map (3, 4). Ephrin-A5 (5) is predominantly expressed in the posterior half of the chick tectum in a steep gradient, whereas a second ephrin, ephrin-A2 (6), is expressed in a shallower gradient across the entire tectum (7), and both gradients exist throughout the formation of the retinotectal map. These expression patterns suggest that ephrin-A5 and ephrin-A2 act in the graded repulsion of retinal axons involved in mapping. This notion is supported by aberrant retinal axon extension beyond their target areas observed in embryos with single and double deletions of the ephrin-A5 and ephrin-A2 genes (8, 9). These genetic deletion studies showed the overall importance of ephrin-A ligands as topographic labels, but how these ligands act *in vivo* has not been demonstrated.

In mammals and avians, the development of topographical order occurs through a multistep process: initial axon outgrowth, topographically specific arborization, and remodeling (10, 11). Initial axon outgrowth is relatively inaccurate, and axons often overshoot beyond their correct termination zone (TZ). Topographically specific branching and arborization in higher vertebrates leads to the initial formation of the map (4) and is thought to be the critical event in map formation (12). Later remodeling by elimination of aberrant arbors refines this map by activity-dependent processes (13). Transient overshooting into the inferior colliculus in ephrin-A5$^{-/-}$ mice (8) demonstrated the repulsive activity of ephrin-A5 on retinal growth cones in the initial outgrowth step *in vivo*. However, these studies were not able to address the role of the ephrin-A5 during the development of arborization, as ephrin-A5 function was lost globally and chronically, and axons were examined only after the retinotectal map was formed. Interpretation of these deletion studies is further confounded by concurrent ephrin expression on retinal ganglion cells (RGCs) in a countergradient to EphA receptors (14–16). To assess the independent guidance role of ephrin-A5 in the tectum, a localized and acute perturbation of ephrin-A gradients in the tectum without changing the expression in RGC axons is required.

Chromophore-assisted laser inactivation (CALI) disrupts the function of a targeted protein both locally and acutely by using a malachite green (MG)-labeled antibody specific to the protein, which is then irradiated with laser light (17, 18). In this study, we performed CALI in the posterior tecta of chick embryos *in vivo* to elucidate how ephrin-A5 acts in retinotopic map formation. By applying this method at specific developmental stages, we show a specific role of ephrin-A5 on the topographic specification of arborization.

Methods

Animals. Fertile chicken eggs were obtained from SPAFAS (Preston, CT) and incubated at 38°C in a humidified incubator. Embryos were exposed for manipulations by creating a window in the shell and then incubated after sealing the hole with transparent tape. Because windowing and other manipulations caused some developmental delay, the developmental stage of the embryos was determined according to Hamburger and Hamilton (19) at the end of each experiment. For analysis of initial outgrowth and arborization, only embryos at stages 37 and 38 which had comparable axon labeling in both tecta were included in the two data sets (E11 and E12, respectively).

CALI of Ephrin-A5 *in Vitro* and Growth Cone Collapse Assay. Ephrin-A5-alkaline phosphatase (AP) (20) incubated with MG-anti-ephrin-A5 (7) or MG-mouse nonimmune IgG (Pierce) in 10-fold molar excess was irradiated with 620-nm laser light (3 min, 15.6

This paper was submitted directly (Track II) to the PNAS office.

Abbreviations: CALI, chromophore-assisted laser inactivation; TZ, termination zone; RGC, retinal ganglion cell; MG, malachite green; AP, alkaline phosphatase; DiI, 1,1′-dioctadecyl-3,3,3′,3′-tetramethylindocarbocyanine perchlorate; SO, stratum opticum; SGFS, stratum griseum et fibrosum superficiale; A–P, anterior–posterior.

†Present address: Brain Science Institute, Institute of Physical and Chemical Research, Wako, Saitama 351-0198, Japan.

‡Present address: Department of Biology, University of Louisville, Louisville, KY 40292.

¶Present address: Medical Research Council Centre for Developmental Neurobiology, King's College London, London SE1 1UL, United Kingdom.

**To whom reprint requests should be addressed. E-mail: daniel.jay@tufts.edu.

NEUROBIOLOGY

mJ/pulse at 10 Hz, 2-mm-diameter spot size) from a pulsed yttrium–aluminum–garnet–neodymium-pumped dye laser (models GCR11 and PDL2, Spectra-Physics). The mixture containing 1 μM ephrin-A5-AP was applied to E7 chick retinal explant culture grown on laminin substrate (21). For time-lapse recording, phase contrast images of growth cones were captured under computer control every 30 s by using a charge-coupled device camera attached to a Nikon Diaphot 200 inverted microscope, starting 10 min before and ending 30 min after application of the solutions. For quantification of the effects of ephrin-A5, growth cones were fixed with 3.7% paraformaldehyde after a 30-min incubation, and lamellipodial areas of randomly selected growth cones were measured with the National Institutes of Health IMAGE program. Only growth cones not in contact with other neurites or cells were included in the data set. Data shown are from three independent experiments.

CALI of Ephrin-A5 *in Vivo*. E10 embryos were used for 1,1′-dioctadecyl-3,3,3′,3′-tetramethylindocarbocyanine perchlorate (DiI) labeling. For position-specific axon labeling, a glass micropipette filled with 10% DiI in dimethyl formamide was inserted into both sides of the dorsotemporal retina through a small hole in the sclera, and DiI was pressure-injected using a Picospritzer II (Parker Hannifin) (11). Forty-two hours later at E12, MG-anti-ephrin-A5 (0.3 mg/ml, 10 μl) was pressure-injected into both sides of the ventricle and subpial space overlying the dorsal tecta. After a 5-hour incubation, the ventro–posterior part of one tectum was subjected to laser irradiation (5 min, 16.8 mJ/pulse). After 11 hours, brains and retinas were exposed and fixed by immersion in 4% paraformaldehyde in PBS at 4°C (10). Whole mounts of the retinas and the tecta on black nitrocellulose membrane were made by appropriate incisions and attached to coverslips with 2.5% diazabicyclo-octane in 0.1 M phosphate buffer (pH 8.0). The Fab fragment of anti-mouse IgG (Jackson ImmunoResearch) was absorbed with an excess amount of immobilized Fab fragment of mouse IgG (Jackson ImmunoResearch), and its specific reaction to Fc fragment of mouse IgG was confirmed by a dot-blot assay. After conjugation with MG, the Fab fragment was preincubated with nonlabeled anti-ephrin-A5 at a 3:1 molar ratio for 1 h and injected in the same way as MG-anti-ephrin-A5. For analyses of the effects on initial axon outgrowth, E9 embryos were used for DiI labeling, and the rest of the experiment was performed in the same way.

Analysis. The whole mounts were observed with a Zeiss Axiovert 10 inverted microscope equipped with epifluorescence optics and a silicon intensified target camera (Hamamatsu) or a Zeiss LSM 410 confocal microscope. To confirm the location of dye injection, retinas were photographed as flat mounts. Although the site of dye injection was slightly variable, there were no obvious correlations in the size or location of the labeling sites that could account for the observed differences in the projections. For analysis of arborization, serial images along the z axis were captured every 5 μm with the confocal microscope or 15 μm with the fluorescence microscope equipped with a 20× objective lens (numerical aperture 0.5). Axonal extension in the stratum opticum (SO) and those branches and arbors proceeding from the SO into deeper laminae in the stratum griseum et fibrosum superficiale (SGFS) were traced. Both imaging methods yielded similar results. Only axons with three or more branches >4 μm in length were considered arbors. At late E12 (stage 38) some arbors are still transient and remain in the more superficial layers with widespread branches (22, 23). To observe the effect of CALI on more mature arbors, only arbors with segments deeper than 50 μm from the surface were subsequently analyzed. After generating a photomontage, the most distal tip of an axon in the superficial layer or a region covered by branches derived from one axon was individually marked, and distances between centroids of the marked region and the termination zone were measured using IPLab software (Scanalytics, Billerica, MA).

EphA3-AP Staining. After CALI of ephrin-A5, tecta were dissected and incubated with 0.3 nM EphA3-AP for 30 min (24). After rinsing, tecta were fixed with 4% paraformaldehyde, and endogenous AP activity was heat inactivated at 65°C for 45 min. Binding activity to EphA3 *in situ* was detected by color development with 5-bromo-4-chloro-3-indolyl phosphate and nitro blue tetrazolium for 15 min (6). Images were recorded with a dissecting microscope (Leica MZFLIII) equipped with a cooled charge-coupled device camera (Hamamatsu, Middlesex, NJ; C4742-95). For densitometry, profile plots of the digitized images were calculated using the National Institutes of Health Image program.

Immunohistochemistry. E10 chick embryos were exposed, subjected to MG-anti-ephrin-A5 injection as described, and incubated for the following 6.5 h. The dissected tecta were rinsed with PBS and fixed in 4% paraformaldehyde. The tecta were then stained with fluorescein-anti-mouse IgG (Cappel) and visualized by fluorescence microscopy.

Results

We tested CALI of ephrin-A5 *in vitro by using* a growth cone collapse assay (21). After conjugation with MG (17), a monoclonal antibody specific for ephrin-A5 (7) was incubated with soluble ephrin-A5-AP (20) and irradiated with 620-nm laser light. This mixture was applied to retinal growth cones growing on a laminin substrate (Fig. 1 *a* and *b*). Without laser irradiation, the mixture caused substantial growth cone collapse and neurite retraction similar to the effect of ephrin-A5 alone (Fig. 1*a*). In contrast, laser irradiation inactivated the ephrin-A5, resulting in unhindered growth cone extension with no sign of collapse (Fig. 1*b*). For quantitative analysis of the collapsing activity, growth cone areas were measured after the 30-min incubation (Fig. 1*c*). MG-anti-ephrin-A5 without laser irradiation did not significantly alter the collapse activity of ephrin-A5. Laser irradiation induced significant inhibition of ephrin-A5 activity by ≈80% ($P < 0.01$, the Student–Newman–Keuls test for multiple comparison). Indeed, the surface area of these growth cones was indistinguishable from the area of control growth cones that did not see ephrin-A5. MG-nonimmune IgG did not show any effect on ephrin-A5 activity regardless of laser irradiation. These findings demonstrate the efficacy of CALI of ephrin-A5 *in vitro*.

We showed that injected antibodies penetrate and bind to ephrin-A5 in tectal tissue by immunohistochemistry. MG-anti-ephrin-A5 was injected into both ventricles through tectal tissue and into the subpial space overlying the tectum. After a 2.5-, 5-, 6.5-, or 16-h incubation period, the tectum was removed, fixed, and stained with FITC-anti-mouse IgG. The staining pattern showed a graded expression along the A–P axis similar to the established expression pattern of ephrin-A5 in the tectum (7) (Fig. 2*a*), whereas sham-injected or MG-IgG-injected embryos showed weak and diffuse staining of the tecta without a detectable gradient (data not shown). A 5-h incubation resulted in saturated fluorescence intensity that was retained beyond 16 h and staining of radial glial fibers throughout the depth of the tectum (7). These findings showed that injection allows for sufficient penetration and specific binding of the MG-anti-ephrin-A5 in tectal tissue.

We tested inactivation of ephrin-A5 in specific loci in the tectum *in vivo* by using a fusion protein containing the extracellular ligand-binding domain of EphA3 receptor and human placental alkaline phosphatase (EphA3-AP) (20) as an affinity probe. Following CALI of ephrin-A5 *in vivo*, dissected tecta were incubated with EphA3-AP, and AP activity was detected

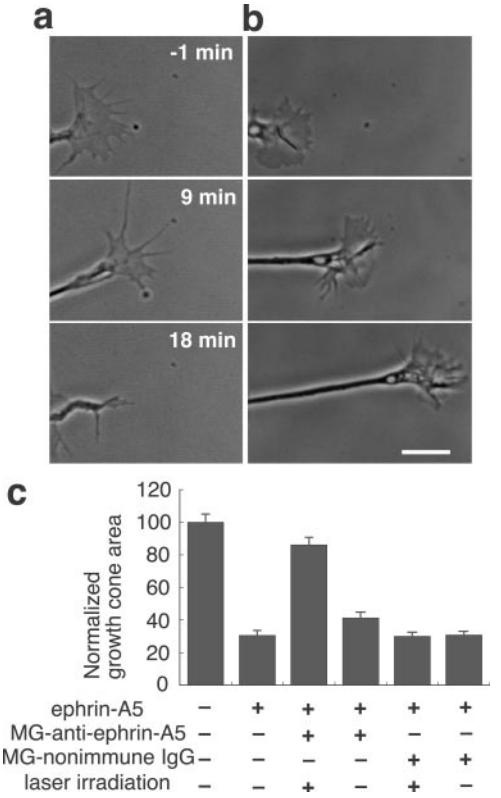

Fig. 1. CALI inactivates soluble ephrin-A5 *in vitro*. (*a* and *b*) Time lapse recording of retinal growth cones. The mixture of ephrin-A5-AP and MG-anti-ephrin-A5 with (*b*) or without (*a*) laser irradiation was applied to retinal growth cones at time 0. (Bar = 10 μm.) (*c*) Collapsing activity of ephrin-A5-AP was inhibited by CALI. Areas of growth cones after treatment were measured (n = 50) and normalized to the average area of control growth cones and expressed as a percentage. Data shown are means + SEM.

colorimetrically. The nonirradiated contralateral tectum showed an unperturbed gradient along the A–P axis similar to the native expression gradient of ephrin-A5 (Fig. 2*b*). In contrast, the laser-irradiated tectum showed specific reduction of binding activity within the laser spot. There was a marked change (42 ± 7%, n = 5) in the gradient pattern of EphA3-AP binding compared with the matched nonirradiated tectum as determined using densitometry (Fig. 2*c*). The remaining binding activity is likely due to the contribution by ephrin-A2, which is unaffected by CALI as the monoclonal antibody used does not bind to ephrin-A2 (7).

We performed several experiments to establish the specificity and time dependence of CALI-mediated loss of ephrin-A5 *in vivo*. We excluded the possibility of nonspecific free radical damage due to the simple binding of MG-labeled antibody to tectal cells by the following experiment. We used an MG-labeled Fab fragment derived from anti-Fc antibody (MG-anti-Fc), and we bound this to an unlabeled anti-ephrin-A5 in a CALI experiment. This serves to localize MG to ephrin-A5 on the tectal membrane but moves it ≈100 Å away from direct binding to ephrin-A5. Inactivation of ephirn-A5 collapsing activity using MG-anti-Fc-anti-ephrin-A5 was reduced by 80%, a value consistent with the established spatial restriction of CALI (18). CALI using MG-anti-Fc-anti-ephrin-A5 on tecta did not affect the EphA3-AP binding gradient and was indistinguishable from MG-nonimmune mouse IgG controls (data not shown). We defined the recovery time after CALI by assaying EphA3-AP binding to the tectum 11 and 17 h after CALI of ephrin-A5. After 11 h, there was still a significant reduction of the binding activity

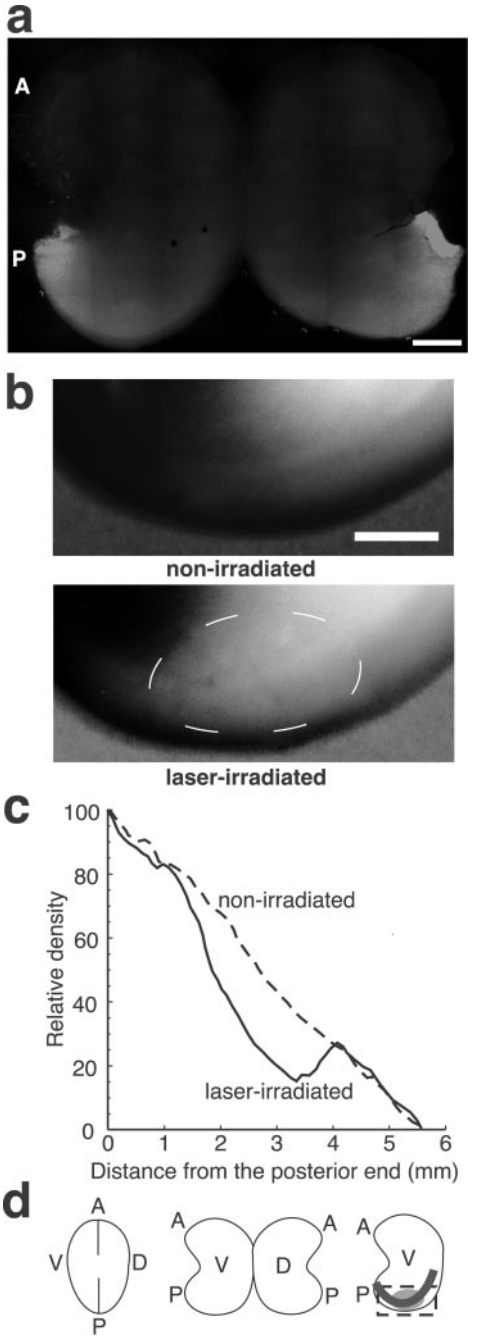

Fig. 2. CALI inactivates ephrin-A5 in the tectum *in vivo*. (*a*) MG-anti-ephrin-A5 is accessible to chick tectal tissue *in vivo*; 6.5 h after injection of MG-anti-ephrin-A5, the tectum was dissected, fixed, and stained with fluorescein-anti-mouse IgG. A similar gradient along the A–P axis to the expression gradient of ephrin-A5 was observed. (Bar = 1 mm.) (*b*) CALI inhibits receptor binding activity *in situ*. Following CALI of ephrin-A5 *in vivo*, dissected tecta were incubated with EphA3-AP, and AP activity was detected by color development. We used E10 embryos in which no axons extend within the posterior tecta to avoid a contribution from nasal axons expressing ephrin-A5 (28). The nonirradiated posterior tectum showed a similar gradient along the A–P axis to the expression gradient of ephrin-A5 in the tectum. However, the laser-irradiated tectum showed reduction of binding activity corresponding to the laser spot (encircled by a thin broken white line). (Bar = 1 mm.) (*c*) Densitometry on the posterior tecta along an A–P axis (illustrated by a thick line in *d*) showed marked decrease of receptor binding activity corresponding to the laser spot *in situ*. (*d*) Schematic drawings of the flat mount of tecta. By incisions along the A–P axis, flat mounts were made. (*Right*) The box illustrates the area shown in *b* and *c*. The ellipse corresponds to the laser spot and shows less color development. A, anterior; P, posterior; V, ventral; D, dorsal.

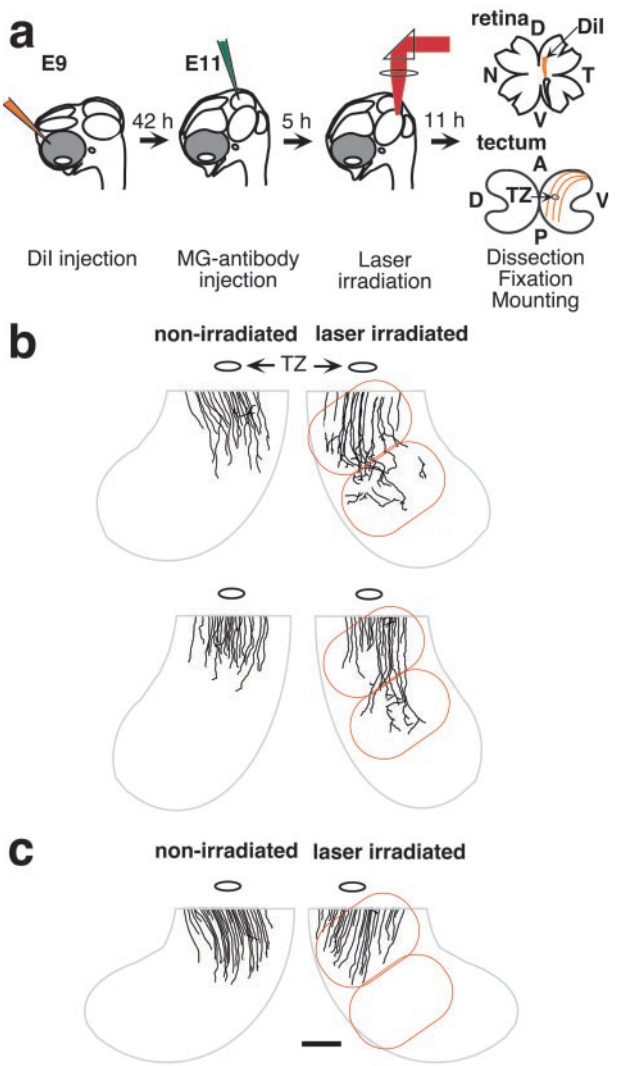

Fig. 3. CALI of ephrin-A5 at E11 increases extension of initial outgrowth in a subset of axons. (*a*) A schematic drawing of experimental procedures. (*b* and *c*) CALI of ephrin-A5 affects retinal axon outgrowth at E11. Typical changes in axonal projections caused by CALI are shown by camera lucida tracings. For clarity, only ventro–posterior quadrants are exhibited, but most axons did not reach the posterior tectum. Nonirradiated tecta (*Left*) demonstrated the normal overshoot beyond the TZ. Some retinal axons in the irradiated area (encircled by red lines) displayed increased extension (*b*). MG-nonimmune IgG-treated tecta did not show such changes in the irradiated area (*c*). (Bar = 1 mm.)

(62% of the initial reduction, $n = 3$) but only 27% ($n = 3$) of the initial reduction was observed after 17 h. Together, these data show that CALI *in vivo* can deplete ephrin-A5 activity in the tectum acutely and locally for at least 11 h.

To elucidate the *in vivo* roles of ephrin-A5 as a positional label in the posterior tectum, we analyzed the change of retinal projections caused by focal inactivation of ephrin-A5 expressed on tectal cells. To label temporal axons that extend into the posterior tectum, we injected DiI into both retinas in positions dorsal and slightly temporal from the midpoint (Fig. 3*a*). During embryo culture *in ovo*, both tecta were injected with MG-anti-ephrin-A5 and incubated for 5 h. One tectum was irradiated with 620-nm laser light on two adjacent 2-mm-diameter spots in the ventro–posterior region where the labeled temporal axons will encounter the ephrin-A5 gradient. After an 11-h incubation, the tecta and retinas were fixed, and retinal axon projections were observed by fluorescence microscopy. Axonal projections in irradiated regions were compared with those in the nonirradiated tectum for each embryo. As controls, MG-nonimmune mouse IgG and MG-anti-Fc-anti-ephrin-A5 were used for CALI, and resulting embryos were analyzed in the same way. There were no observable changes in axon projections caused by laser irradiation or MG-antibody injections alone (data not shown).

We confirmed that ephrin-A5 prevents axon overshoot and that CALI of ephrin-A5 in E11 chicks can diminish this functional role. On the control tecta, many labeled axons passed through the topographically correct TZ and may occasionally overshoot up to 2 mm from the TZ (Fig. 3*b Left*). Some axons start to make rudimentary arbors preferentially around the TZ, but few branch into the posterior half of tecta. In contrast, when CALI of ephrin-A5 was performed, we observed greater extension beyond the usual limit with overshoot of up to 4 mm from the TZ (six of eight embryos). Fig. 3*b* (*Right*) shows two examples of these findings. At this stage (early 37), most growth cones of labeled axons were still in the anterior tectum (not shown). Not all labeled axons in the posterior tectum showed abnormal extensions. This may be due to the activity of ephrin-A2 that may have overlapping function in restricting initial axon outgrowth. Alternatively, the effect of CALI of ephrin-A5 may be limited to a specific developmental stage of axonal projection or on a specific subgroup of retinal axons. CALI using MG-nonimmune IgG ($n = 6$) or using MG-anti-Fc-anti-ephrin-A5 ($n = 4$) had no effect on axonal projections (Fig. 3*c*).

Interestingly, we observed no effect on axon extension in the superficial tectal layer when CALI of ephrin-A5 was performed at E12. A typical example is shown in Fig. 4*a* by tracing of labeled axons in the superficial layer in the posterior tecta. The extent of axon outgrowth on the irradiated area was indistinguishable from that seen on the nonirradiated side. For quantitative analysis, positions of axonal tips in the superficial layer were marked, and the distances along the A–P axis from the center of the TZ were measured. At this stage, the TZ was easily distinguished as a well defined area with deeper and fine arborization in the topographically appropriate part expected from the injected position in the retinas. In pairwise comparisons between irradiated and nonirradiated sides, five of six tecta treated with CALI of ephrin-A5 did not show statistically significant differences in the relative axonal tip location (Mann–Whitney rank sum test). A comparison of embryos subjected to CALI of ephrin-A5 with all controls did not show significant changes in locations of the axonal tips relative to the TZ (Dunn's test for multiple comparison, $P < 0.01$, Fig. 4 *b* and *c*). Controls included tecta injected with MG-anti-ephrin-A5 (without irradiation), MG-nonimmune IgG, or MG-anti-Fc-anti-ephrin-A5. These findings show that ephrin-A5 restricts axon overshoot during the period of initial outgrowth (E11) but has no effect on overshoot by late E12, after initial outgrowth is mostly completed.

Thus far, it has been difficult to demonstrate ephrin-A5 in back branching and arborization *in vivo* (10, 11), although *in vitro* studies have suggested a role for ephrin-A family members (12). We tested a specific role of ephrin-A5 in limiting arborization *in vivo* by performing CALI of ephrin-A5 with late E12 embryos, the stage when arborization in deeper layers begins (23) but before activity-dependent refinement (13). At this developmental stage, most of the axons have reached their maximal extension in the most superficial layer, the SO, up to 2 mm beyond the TZ. The map is then established by perpendicular arborization (23) to topographically correct sites (4) in deeper layers in the SGFS. At this stage, ephrin-A5 is mainly expressed on radial glia (especially endfeet in the SO) (7) and possibly on processes of tectal neurons (25, 26).

We analyzed the effect of CALI of ephrin-A5 on the arborization into the SGFS layer (Fig. 5*a*). Confocal microscopy of this layer revealed that arbors in nonirradiated tecta were mainly

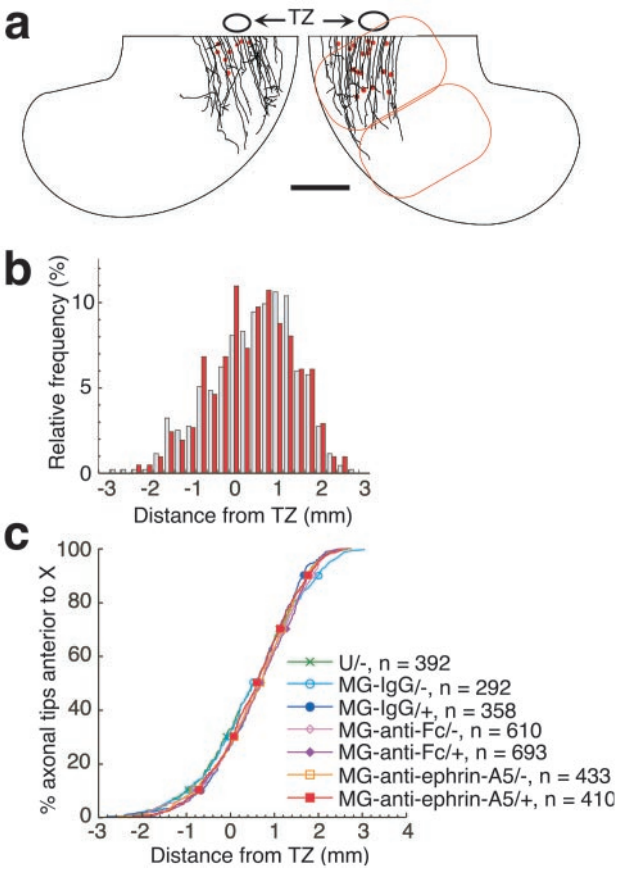

Fig. 4. CALI of ephrin-A5 at E12 does not increase axonal extension in the SO. (*a*) CALI of ephrin-A5 does not affect retinal axon outgrowth in the SO. A typical example of axonal projections in the SO is shown by camera lucida tracings. For clarity, only ventro–posterior quadrants are exhibited. Red dots show positions of arbors in the layers deeper than 50 μm. (Bar = 1 mm.) (*b*) A relative histogram showing the distribution of axonal tips along the A–P axis in laser-irradiated (red) and nonirradiated (blue) tecta treated with MG-anti-ephrin-A5. (*c*) An analysis of changes in locations of axonal tips after CALI. The plot depicts the distribution of axonal tips along the A–P axis; values given on the *y* axis indicate the proportion of axons that did not reach the positions shown on the *x* axis. No significant changes were observed.

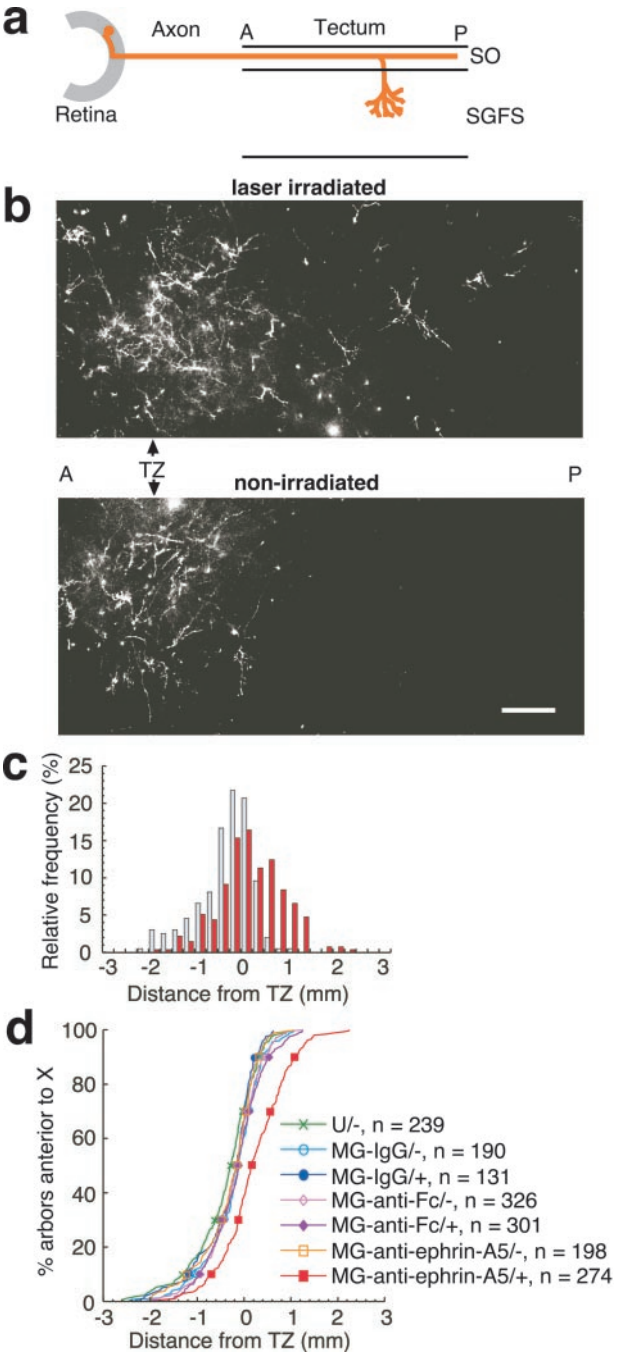

Fig. 5. CALI of ephrin-A5 at E12 causes a posterior shift of arbors. (*a*) A schematic drawing to show arbor formation in tecta. Most of the labeled axons have reached their maximal extension in the SO and extend into deeper layers in the SGFS by branching. (*b*) Arbor formation in the layers deeper than 50 μm from the tectal surface visualized by confocal microscopy. Several *z* axis series images in the same field were combined by summation. The montages show DiI-labeled axonal arbors around and posterior to the TZ in the laser-irradiated tectum (*Upper*) but only around the TZ in the nonirradiated tectum (*Lower*). (Bar = 200 μm.) (*c*) A relative histogram showing the distribution of arbors along the A–P axis in laser-irradiated (red) and nonirradiated (blue) tecta treated with MG-anti-ephrin-A5. Whereas arbor formation in nonirradiated tecta treated with MG-anti-ephrin-A5 is relatively restricted to the topographically correct TZ, RGC axons in the irradiated area showed ectopic arbor formation posterior to the TZ. (*d*) An analysis of changes in arbor localization after CALI. The plot delineates the relative distribution to the TZ of deep arbors along the A–P axis in the same way as Fig. 4*c*. Only the laser-irradiated tecta treated with MG-anti-ephrin-A5 showed a significant posterior shift. *, $P < 0.01$ by Dunn's test for multiple comparison.

localized around the TZ with marked preference for topographically correct sites in control embryos (Fig. 5*b Lower*). In contrast, CALI of ephrin-A5 caused a marked shift of arbor localization posterior to the TZ (Fig. 5*b Upper*). A histogram of the position of arbors shows this shift graphically (Fig. 5*c*). All six tecta treated with CALI of ephrin-A5 showed statistically significant shifts in arbor distribution compared with the matched nonirradiated controls (Mann–Whitney rank sum test, $P < 0.05$). In contrast, none of tecta treated with CALI using MG-nonimmune IgG ($n = 3$) or MG-anti-Fc-anti-ephrin-A5 ($n = 4$) showed such significant shifts. This last control is particularly stringent because it localizes an MG-labeled antibody directly to ephrin-A5 but at a distance (≈100 Å based on the size of an IgG molecule) beyond the spatial restriction of the effects of CALI (15 Å) (18). Pooling the data of relative locations of the arbors with respect to the TZ showed that only CALI of ephrin-A5 caused a statistically significant effect (Dunn's test for multiple comparison, $P < 0.01$, Fig. 5*d*). These findings show that the local loss of ephrin-A5 in the posterior tectum causes ectopic arborization in the deeper layers. The posterior shift of arborization without a change in the initial axon outgrowth step clearly shows that the arborization step is independently controlled by ephrin-A5.

Discussion

Recent studies have shown that topographic-specific arborization is the critical event in forming the retinotopic map (12). Genetic deletion studies demonstrated that ephrin-A2 and ephrin-A5 restrict initial axon outgrowth (9), but analyses of topographically specific arborization caused by changes of ephrin-A gradients *in vivo* had not been performed because of lack of appropriate approaches. Previous studies could also not differentiate between a direct role of ephrin-A5 on arborization and modifications by activity-dependent remodeling. Furthermore, a specific role for ephrin-A5 in the tectum could not be distinguished from potential roles elsewhere (such as in the retina or the optic nerve). Indeed, previous studies have shown expression of ephrin-A5 in retinal ganglion cells and functional modulation of EphA receptor function by this expression (14). Direct evidence for the molecules that regulate retinotectal arborization has been lacking, although *in vitro* studies have suggested that the repulsive activity of ephrin-A ligands may serve this role. EphA3-Fc binds to ephrin A ligands to inhibit their function, and this interferes with temporal axon branching from retinal explants in a modified stripe assay (12). By using an RGC-tectal cell coculture system, Davenport *et al.* (27) showed an intriguing phenomenon that sprouting of branches from trailing axons was induced several hundred micrometers behind the collapse site of leading axons by ephrin-A ligands. This sprouting might be a fundamental *in vivo* mechanism for topographically specific branching. Axons are thought to contact with radial glial fibers that express ephrin-A5 during branch formation to sense the positional information (22).

Ephrin-A5 has been inactivated *in vivo* by using a nongenetic strategy, and the data serve as an independent confirmation of ephrin-A5's role in restricting initial RGC axon outgrowth on the tectal surface. CALI eliminated function of ephrin-A5 in a subregion of the tectum at specific developmental stage. This has allowed us to show changes in topographically specific arborization caused by inactivation of ephrin-A5 in the tectum without modifications caused by the following remodeling step (13) or changes in ephrin-A5 expressed in the retina. Thus, we have shown that ephrin-A5 serves as a key determinant in the tectum for topographically specific arborization. This, coupled with the established role for ephrin-A5 in restricting initial axon outgrowth, suggests a double mechanism for ephrin-A5 in retinotectal map formation. Graded ephrin-A5 expression stops growth cone advance on the surface of the posterior tectum. Based on *in vitro* studies, ephrin-A5 may also trigger the formation of secondary arbors along the primary axon that dive to the deeper tectal layers (27). These arbors define the retinotopic map in the SFGS where ephrin-A5 acts again to restrict the topographically correct positions that will then be later refined by activity-dependent processes. Previous studies have suggested roles for ephrin-A5 in branching or in topographic axon guidance (8, 12). The differential timing of application of CALI of ephrin-A5 has shown when and where these functions are required.

Our findings also provide a proof of principle of CALI as a genetically independent strategy to address *in vivo* function in higher vertebrates that is capable of timed local functional inactivation. Indeed, methods to generate acute and localized loss of function in vertebrate animal model systems are scarce. Whereas our previous studies have shown *in vivo* applications of CALI to be effective for invertebrate model systems, these experiments apply direct protein inactivation to targeted tissues in a higher vertebrate. This approach provides a spatial and temporal resolution in addressing *in vivo* function and may thus have wide application. For example, RGM, a third repulsive cue, has already been inactivated by CALI for *in vitro* studies (29). It would be interesting to address the role of RGM *in vivo* alone or in combination with ephrin-A5 and A2. All inactivation strategies (genetic knockout included) require complementary confirmation, and CALI provides this. This said, it is also clear that conclusions drawn from CALI-based experiments also need support from independent approaches. As each approach provides information that is specific for the disruption caused (e.g., acute vs. chronic; local vs. global), applying different approaches together provide greater confidence in conclusions of *in vivo* function.

We thank Friedrich Bonhoeffer for helpful discussion and an unknown reviewer for helpful comments. This work was supported by National Institutes of Health Grants EY11992 and NS34699 (to D.G.J.).

1. Sperry, R. W. (1963) *Proc. Natl. Acad. Sci. USA* **50,** 703–710.
2. Mueller, B. K. (1999) *Annu. Rev. Neurosci.* **22,** 351–388.
3. Flanagan, J. G. & Vanderhaeghen, P. (1998) *Annu. Rev. Neurosci.* **21,** 309–345.
4. O'Leary, D. D., Yates, P. A. & McLaughlin, T. (1999) *Cell* **96,** 255–269.
5. Drescher, U., Kremoser, C., Handwerker, C., Loschinger, J., Noda, M. & Bonhoeffer, F. (1995) *Cell* **82,** 359–370.
6. Cheng, H. J., Nakamoto, M., Bergemann, A. D. & Flanagan, J. G. (1995) *Cell* **82,** 371–381.
7. Monschau, B., Kremoser, C., Ohta, K., Tanaka, H., Kaneko, T., Yamada, T., Handwerker, C., Hornberger, M. R., Loschinger, J., Pasquale, E. B., *et al.* (1997) *EMBO J.* **16,** 1258–1267.
8. Frisen, J., Yates, P. A., McLaughlin, T., Friedman, G. C., O'Leary, D. D. & Barbacid, M. (1998) *Neuron* **20,** 235–243.
9. Feldheim, D. A., Kim, Y.-I., Bergemann, A. D., Frisen, J., Barbacid, M. & Flanagan, J. G. (2000) *Neuron* **25,** 563–574.
10. Nakamura, H. & O'Leary, D. D. (1989) *J. Neurosci.* **9,** 3776–3795.
11. Simon, D. K. & O'Leary, D. D. (1992) *J. Neurosci.* **12,** 1212–1232.
12. Yates, P. A., Roskies, A. L., McLaughlin, T. & O'Leary, D. D. (2001) *J. Neurosci.* **21,** 8548–8563.
13. Wong, W. T., Sanes, J. R. & Wong, R. O. (1998) *J. Neurosci.* **18,** 8839–8852.
14. Hornberger, M. R., Dütting, D., Ciossek, T., Yamada, T., Handwerker, C., Lang, S., Weth, F., Huf, J., Wessel, R., Logan, C., *et al.* (1999) *Neuron* **22,** 731–742.
15. Dütting, D., Handwerker, C. & Drescher, U. (1999) *Dev. Biol.* **216,** 297–311.
16. McLaughlin, T. & O'Leary, D. D. (1999) *Neuron* **22,** 636–639.
17. Beermann, A. E. & Jay, D. G. (1994) *Methods Cell Biol.* **44,** 715–732.
18. Wang, F.-S. & Jay, D. G. (1996) *Trends Cell Biol.* **6,** 442–445.
19. Hamburger, V. & Hamilton, H. L. (1951) *J. Morphol.* **88,** 49–92.
20. Ciossek, T., Monschau, B., Kremoser, C., Loschinger, J., Lang, S., Muller, B. K., Bonhoeffer, F. & Drescher, U. (1998) *Eur. J. Neurosci.* **10,** 1574–1580.
21. Cox, E. C., Muller, B. & Bonhoeffer, F. (1990) *Neuron* **4,** 31–37.
22. Vanselow, J., Thanos, S., Godement, P., Henke-Fahle, S. & Bonhoeffer, F. (1989) *Dev. Brain Res.* **45,** 15–27.
23. Yamagata, M. & Sanes, J. R. (1995) *Development (Cambridge, U.K.)* **121,** 189–200.
24. Braisted, J. E., McLaughlin, T., Wang, H. U., Friedman, G. C., Anderson, D. J. & O'Leary, D. D. (1997) *Dev. Biol.* **191,** 14–28.
25. Davenport, R. W., Thies, E., Zhou, R. & Nelson, P. G. (1998) *J. Neurosci.* **18,** 975–986.
26. Davenport, R. W. (1997) *Cell Tissue Res.* **290,** 201–208.
27. Davenport, R. W., Thies, E. & Cohen, M. L. (1999) *Nat. Neurosci.* **2,** 254–259.
28. Goldberg, S. (1974) *Dev. Biol.* **36,** 24–43.
29. Mueller, B. K., Jay, D. G. & Bonhoeffer, F. (1996) *Curr. Biol.* **6,** 1497–1502.